SMAR 2019 – Fifth Conference on Smart Monitoring,
Assessment and Rehabilitation of Civil Structures

SMAR 2019

Improvement of FeMnSi based shape memory alloys yield stress by heat treatment

Yajiao YANG [1, 2], Ariyan ARABI-HASHEMI [3], Christian LEINENBACH [3],
Moslem SHAHVERDI [1]

[1] Structural Engineering Laboratory, Empa, Dübendorf, Switzerland

[2] Laboratory for Multifunctional Ferroic Materials, ETH, Zürich, Switzerland

[3] Laboratory for Advanced Materials Processing, Empa, Dübendorf, Switzerland

Contact e-mail: moslem.shahverdi@empa.ch

ABSTRACT: Iron-based shape memory alloys (Fe-SMAs) attract more and more attention in recent years. The improvement of the shape memory effect (SME), i.e. recovery strain, has been extensively studied. In civil engineering, Fe-SMAs can be used as pre-stressing elements for concrete structures. For this application, recovery stress of Fe-SMAs is an essential characteristic to evaluate the reinforcement ability and therefore, large value is preferred. However, it is acknowledged that high recovery strain does not always correspond to high recovery stress. Investigation to improve recovery stress of Fe-SMAs is demanding in real application. High yield stress and SME are beneficial to achieve high recovery stress, and these two factors are strongly dependent on the aging conditions for the FeMnSi with precipitates type shape memory alloy. This paper investigates the influence of different aging conditions on the yield stress and pseudoelasticity ε_{pe} of the Fe-SMA. It is shown that the maximum 0.1% yield stress reaches up to 670 MPa upon aging at 600°C for 72h waiting.

Keywords: iron-based shape memory alloy; FeMnSi based shape memory alloy; heat treatment; yield stress; pseudoelasticity; recovery stress.

1 INTRODUCTION

A SMA (shape memory alloy) has the ability to return to its initial shape after deformation. Compared to nickel-titanium shape memory alloys (NiTi-SMAs), Fe-SMAs are cost-effective and easily manufactured, and therefore are becoming more and more popular in civil engineering, e.g. Sawaguchi et al. (2006), Shahverdi et al. (2016), Shahverdi et al. (2017), Michels et al. (2018) and Shahverdi et al. (2018).

1.1 Recovery strain and recovery stress

Recovery strain of Fe-SMAs, is the recovered strain of deformed Fe-SMAs after heating and cooling. In this case, the Fe-SMA is free at its two ends, i.e. the external force applied to Fe-SMA is equal to zero during heating and cooling. The enhancement of recovery strain has been extensively studied, e.g. Otsuka et al. (1990), Wen et al. (2014), Ogawa et al. (1993), Baruj et al. (2002) and Liu et al. (2003), and the conditions for achieving great recovery strain is summarized in Peng et al. (2018).

Recovery stress of Fe-SMAs, on the other hand, is obtained by keeping strain constant during heating and cooling, i.e. the two ends of Fe-SMA are fixed. The final axial stress is called recovery stress and the heating and cooling process is called activation. More detail information about the recovery stress can be found in Shahverdi et al. (2018). Unlike enhancement of

recovery strain, only high SME cannot correspond to high recovery stress. Due to the bending of the stress-temperature curve during cooling, an approach to achieve a higher recovery stress is increasing the yield stress.

Existing studies related to recovery stress improvement are mainly about the alloy composition and thermal-mechanical treatment. According to Wen et al. (2005) and Wen et al. (2007), carbon content plays an important role in recovery stress enhancement since it cannot only increase SMA yield stress but also decrease the martensite start temperature (M_S) and prevent martensitic phase transformation during cooling. Similarly, nitrogen content can also increase SMA yield stress and improve recovery stress, e.g. Ullakko et al. (1996), Ariapour et al. (1999) and Li et al. (2013). In addition, different thermo-mechanical treatment conditions can influence the texture, second phase (precipitates) and dislocation distribution, etc. of the Fe-SMAs and consequently the recovery stress, e.g. Baruj et al. (2002) and Wang et al. (2011).

Besides the mentioned factors, experimental factors (the Fe-SMAs thickness, cutting position, machine preload, pre-straining and maximum heating temperature) were also investigated in Shahverdi et al. (2018). It was found that for the Fe-SMAs with the composition of Fe-17Mn-5Si-10Cr-4Ni-1(V, C) (mass %), 2% or 4% pre-straining is optimal value to achieve higher recovery stress.

1.2 The influence of heat treatment on Fe-SMAs

Since the first Fe-30Mn-1Si single crystal was discovered by Sato et al. (1982), different types of Fe-SMAs emerged in the past few decades. Basically, they can be classified into two types. The first type is the FeMnSi based shape memory alloy, whose SME is enhanced mainly by 'training' or simple thermo-mechanical treatment, e.g. Stanford et al. (2010), Baruj et al. (2008) and Kajiwara et al. (2001), since a large density of stacking faults is produced during the treatment due to Baruj et al. (2008). The second type is FeMnSi with precipitates (niobium carbides, vanadium carbides and vanadium nitrides). Compared to the first type, in Kajiwara et al. (2001), the precipitates can act as nucleation sites for the martensite transformation and therefore enhance the SME. As reported by Sagaradze et al. (2006) and Sagaradze et al. (2008), after solution treatment which aims to homogenize Fe-SMAs by heating, different aging conditions can influence the SME and the yield stress of Fe-SMA significantly. The SME can be improved by overaging while SMA can be strengthened by precipitation hardening. Since yield stress and SME are two factors for enhancement of the recovery stress, the recovery stress is expected to be improved by certain aging condition.

Recently, Arabi-Hashemi (2018) proved this assumption by investigating the effect of different aging time at two different temperatures of 630 °C and 830 °C on the recovery stress of the Fe-SMA with the composition of Fe-17Mn-5Si-10Cr-4Ni-1(V, C) (mass %). It was found that the Fe-SMA can achieve recovery stress of 564 MPa by aging at 630 °C without any other thermo-mechanical steps, e.g. cold or hot rolling. In this case, the high recovery stress is achieved only by pre-straining to 2% and low activation temperature of 160 °C. The reason for this high recovery stress is that the SMA is strengthened through precipitation hardening at a low aging temperature and SME keeps a moderate value. Also in 2018, in Lai et al. (2018), it was found that, for the Fe-SMA with the composition of Fe-28Mn-6Si-5Cr-0.764V-0.18C (wt. %), the microstructures are different at different aging temperatures. At low temperature (650 °C), the Fe-SMA mainly consists of dislocations and very fine vanadium carbides. However, at high temperature (higher than 700 °C), the Fe-SMA contains mainly stacking faults and larger carbides. On the base of Arabi-Hashemi's work, the aim of current paper is to further

investigate the effect of other aging temperatures on the SMA yield stress and pseudoelasticity ε_{pe} (the definition can be seen in 3.1 section).

2 EXPERIMENTS

Specimens (provided by re-fer AG) with the composition of Fe-17Mn-5Si-10Cr-4Ni-1(V, C) (mass %) were cut into strips with length of 200 mm, width of 10 mm and thickness of 1.5 mm. The test was conducted by the following procedures: step 1, all specimens were heated to 1070°C and held for 2 h (solution treatment) followed by water quenching; step 2, specimens were aged at 600°C from 2 h to 6 days, or at 774°C from half an hour to 8 h (steps 1 and 2 were conducted on an air furnace); step 3, the mechanical test was conducted on a Z020 Zwick tensile testing machine and the evolution of parameters (strain, stress, etc.) was recorded by the textXpertII Software.

3 RESULTS AND DISCUSSION

3.1 0.1% yield stress and the pseudoelasticity

An example of the stress-strain curve for a tensile test can be seen in Figure 1, which is the result of the specimen aging at 774 °C for 1 h. The 0.1% yield stress can be found at the black point, which is the intersection of the stress-strain curve and the dashed line. The dashed line has the same slope as the Young's modulus and the intersection of it with x-axis is equal to 0.1% strain.

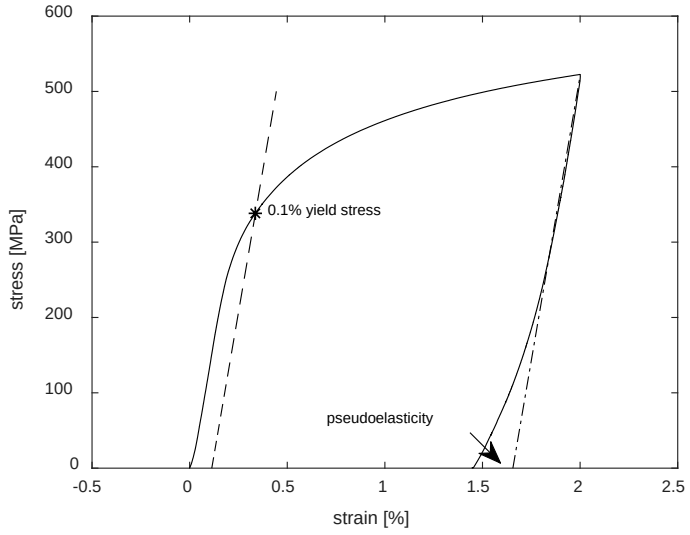

Figure 1 Typical stress-strain curve for tensile test of Fe-SMA strip (aging at 774 °C for 1 h).

During unloading, the stress-strain curve deviates from a straight line. The deviated strain is the pseudoelasticity ε_{pe}, which is due to the combination of back transformation from hexagonal close-packed (hcp) to face-centered cubic (fcc) and a reversible motion of Schockley partial dislocations, e.g. Baruj et al. (2010) and Leinenbach et al. (2017). The ε_{pe} can provide indications of the amount of hcp martensite formed during loading and the SME.

3.2 Aging at 600 °C and 774 °C.

After solution treatment, specimens were aged at 600°C from 2 h to 144 h (6 days), and at 774°C from 0.5 h to 8 h. The 0.1% yield stress and the pseudoelasticity ε_{pe} as a function of aging time can be found in Figure 2 (aging at 600 °C) and Figure 3 (aging at 774 °C). Aging time 0 h means the specimen only underwent solution treatment. The ε_{pe} below 0.1% is too small and can be ignored.

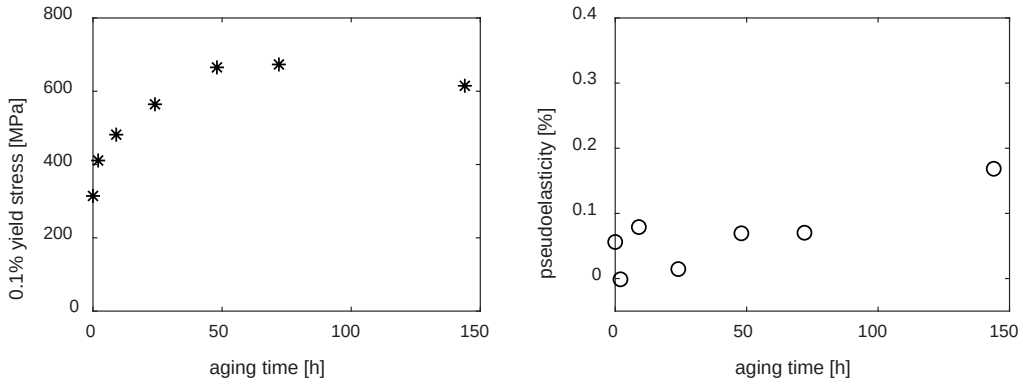

Figure 2 The 0.1% yield stress (left) and the pseudoelasticity ε_{pe} (right) versus aging time (aging at 600°C).

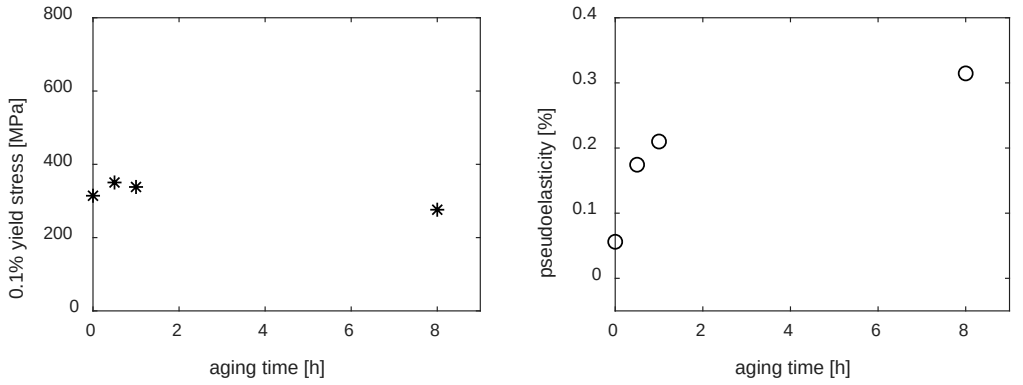

Figure 3 The 0.1% yield stress (left) and the pseudoelasticity ε_{pe} (right) versus aging time (aging at 774°C).

At low temperature (600°C) aging, as the aging time increases from 0 h to 72 h (3 days), the 0.1% yield stress first increases from about 300 MPa to 670 MPa (maximum) and the pseudoelasticity ε_{pe} keeps a very low value (below 0.1%). As the aging time further increases from 72 h to 144 h, the 0.1% yield stress decreases while the ε_{pe} rises up to about 0.2%. Similarly, at high temperature (774°C) aging, the 0.1% yield stress first increases with aging time, reaches its maximum and then decreases. At the same time, the ε_{pe} is below 0.1% at the beginning of aging and rises up to about 3% after waiting for 8h.

During aging of the Fe-SMA, according to Arabi-Hashemi et al. (2018), second phase/precipitate is the main factor to affect the yield stress and pseudoelasticity ε_{pe} . Precipitates formation consists of nucleation and growth, which are temperature and time dependent. At higher temperature (774°C), the energy barrier for nucleation is larger and results in a small number of precipitates. However, the diffusion is faster and leads to larger dimension

of precipitates. As a result, less precipitates with larger size are preferred at higher temperature. On the contrary, more precipitates with smaller size are preferred at lower temperature (e.g. 600°C).

At the beginning of aging, the precipitate number is increasing upon longer aging duration and results in the increment of yield stress due to Orowan mechanism. As the aging time further increases, the precipitates start to coarsen, which results in a decline of the yield stress. It should be noted that only when the precipitate dimension exceeds a certain value, the SME can be improved. This is because fine particles can hinder the martensite transformation. It is found that this value is 50 nm for NbC in Stanford et al. (2008) and 21 nm for VC particles in Lai et al. (2018), respectively. This is the reason that the ε_{pe} increases upon longer duration.

4 CONCLUSION

The influence of different aging conditions on the yield stress and the pseudoelasticity ε_{pe} was studied for the Fe-SMA with the composition of Fe-17Mn-5Si-10Cr-4Ni-1(V, C) (mass %). It was found that the yield stress and pseudoelasticity were strongly affected by aging temperature and time. On one hand, the yield stress could be improved by precipitation hardening. The maximum 0.1% yield stress was about 670 MPa upon aging at 600°C for 72 h. On the other hand, the SME could be improved by overaging.

5 ACKNOWLEDGEMENTS

This study was part of a PhD project, financially supported by the China Scholarship Council (CSC), the Engineering Sciences department at Empa, the Company BÖHLER Edelstahl GmbH in Austria, and company re-fer AG in Switzerland.

6 REFERENCE

Arabi-Hashemi, A., Lee, W. J., and Leinenbach, C. (2018). Recovery stress formation in FeMnSi based shape memory alloys: Impact of precipitates, texture and grain size. *Materials & Design*, *139*, 258-268.

Ariapour, A., Yakubtsov, I., and Perovic, D. D. (1999). Effect of nitrogen on shape memory effect of a Fe–Mn-based alloy. *Materials Science and Engineering: A*, *262*(1-2), 39-49.

Baruj, A., Kikuchi, T., Kajiwara, S., and Shinya, N. (2002). Effect of pre-deformation of austenite on shape memory properties in Fe-Mn-Si-based alloys containing Nb and C. *Materials Transactions*, *43*(3), 585-588.

Baruj, A., Kikuchi, T., Kajiwara, S., and Shinya, N. (2002). Effect of pre-deformation of austenite on shape memory properties in Fe-Mn-Si-based alloys containing Nb and C. *Materials Transactions*, *43*(3), 585-588.

Baruj, A., and Troiani, H. E. (2008). The effect of pre-rolling Fe–Mn–Si-based shape memory alloys: mechanical properties and transmission electron microcopy examination. *Materials Science and Engineering: A*, *481*, 574-577.

Baruj, A., Bertolino, G., and Troiani, H. E. (2010). Temperature dependence of critical stress and pseudoelasticity in a Fe–Mn–Si–Cr pre-rolled alloy. *Journal of alloys and compounds*, *502*(1), 54-58.

Druker, A., Baruj, A., and Malarría, J. (2010). Effect of rolling conditions on the structure and shape memory properties of Fe–Mn–Si alloys. *Materials characterization*, *61*(6), 603-612.

Kajiwara, S., Liu, D., Kikuchi, T., and Shinya, N. (2001). Remarkable improvement of shape memory effect in Fe-Mn-Si based shape memory alloys by producing NbC precipitates. *Scripta materialia*, *44*(12), 2809-2814.

Lai, M. J., Li, Y. J., Lillpopp, L., Ponge, D., Will, S., and Raabe, D. (2018). On the origin of the improvement of shape memory effect by precipitating VC in Fe–Mn–Si-based shape memory alloys. *Acta Materialia*, *155*, 222-235.

Leinenbach, C., Arabi-Hashemi, A., Lee, W. J., Lis, A., Sadegh-Ahmadi, M., Van Petegem, S., and Van Swygenhoven, H. (2017). Characterization of the deformation and phase transformation behavior of VC-free and VC-containing FeMnSi-based shape memory alloys by in situ neutron diffraction. *Materials Science and Engineering: A*, *703*, 314-323.

Li, K., Dong, Z., Liu, Y., and Zhang, L. (2013). A newly developed Fe-based shape memory alloy suitable for smart civil engineering. *Smart Materials and Structures*, *22*(4), 045002.

Liu, D. Z., Kajiwara, S., Kikuchi, T., and Shinya, N. (2003). Atomic force microscopy study on microstructural changes by'training'in Fe-Mn-Si-based shape memory alloys. *Philosophical Magazine*, *83*(25), 2875-2897.

Michels, J., Shahverdi, M., and Czaderski, C. (2018). Flexural strengthening of structural concrete with iron-based shape memory alloy strips. *Structural Concrete*, *19*(3), 876-891.

Ogawa, K., and Kajiwara, S. (1993). HREM study of stress-induced transformation structures in an Fe–Mn–Si–Cr–Ni shape memory alloy. *Materials Transactions, JIM*, *34*(12), 1169-1176.

Otsuka, H., Yamada, H., Maruyama, T., Tanahashi, H., Matsuda, S., and Murakami, M. (1990). Effects of alloying additions on Fe-Mn-Si shape memory alloys. *ISIJ international*, *30*(8), 674-679.

Peng, H., Wang, G., Wang, S., Chen, J., MacLaren, I., and Wen, Y. (2018). Key criterion for achieving giant recovery strains in polycrystalline Fe-Mn-Si based shape memory alloys. *Materials Science and Engineering: A*, *712*, 37-49.

Sawaguchi, T., Kikuchi, T., Ogawa, K., Kajiwara, S., Ikeo, Y., Kojima, M., and Ogawa, T. (2006). Development of prestressed concrete using Fe–Mn–Si-based shape memory alloys containing NbC. *Materials transactions*, *47*(3), 580-583.

Sagaradze, V. V., Belozerov, E. V., Mukhin, M. L., Zainutdinov, Y. R., Pecherkina, N. L., and Zavalishin, V. A. (2006). A new approach to creation of high-strength austenitic steels with a controlled shape-memory effect. *The Physics of Metals and Metallography*, *101*(5), 506-512.

Sagaradze, V. V., Voronin, V. I., Filippov, Y. I., Kazantsev, V. A., Mukhin, M. L., Belozerov, E. V., and Popov, A. G. (2008). Martensitic transformations γ-ε (α) and the shape-memory effect in aging high-strength manganese austenitic steels. *The Physics of Metals and Metallography*, *106*(6), 630-640.

Sagaradze, V. V., Kositsyna, I. I., Mukhin, M. L., Belozerov, Y. V., and Zaynutdinov, Y. R. (2008). High-strength precipitation-hardening austenitic Fe–Mn–V–Mo–C steels with shape memory effect. *Materials Science and Engineering: A*, *481*, 747-751.

Sato, A., Chishima, E., Soma, K., and Mori, T. (1982). Shape memory effect in γ⇄ ϵ transformation in Fe-30Mn-1Si alloy single crystals. *Acta Metallurgica*, *30*(6), 1177-1183.

Shahverdi, M., Czaderski, C., and Motavalli, M. (2016). Iron-based shape memory alloys for prestressed near-surface mounted strengthening of reinforced concrete beams. *Construction and Building Materials*, *112*, 28-38.

Shahverdi, M., Michels, J., Czaderski, C., Arabi-Hashemi, A., and Motavalli, M. (2017). Iron-based shape memory alloy strips, part 1: characterization and material behavior. In SMAR proceedings. Proceedings of SMAR 2017, fourth conference on smart monitoring, assessment and rehabilitation of civil structures (p. 118 (8 pp.). Zurich, Switzerland.

Shahverdi, M., Czaderski, C., Annen, P., and Motavalli, M. (2016). Strengthening of RC beams by iron-based shape memory alloy bars embedded in a shotcrete layer. *Engineering Structures*, *117*, 263-273.

Shahverdi, M., Michels, J., Czaderski, C., and Motavalli, M. (2018). Iron-based shape memory alloy strips for strengthening RC members: Material behavior and characterization. *Construction and Building Materials*, *173*, 586-599.

Stanford, N. and Dunne, D. P. (2006). Thermo-mechanical processing and the shape memory effect in an Fe–Mn–Si-based shape memory alloy. *Materials Science and Engineering: A*, *422*(1-2), 352-359.

Stanford, N., Dunne, D. P., and Li, H. (2008). Re-examination of the effect of NbC precipitation on shape memory in Fe–Mn–Si-based alloys. *Scripta materialia*, *58*(7), 583-586.

Ullakko, K., Jakovenko, P. T., and Gavriljuk, V. G. (1996). High-strength shape memory steels alloyed with nitrogen. *Scripta materialia*, *35*(4), 473-478.

Wang, C. P., Wen, Y. H., Peng, H. B., Xu, D. Q., and Li, N. (2011). Factors affecting recovery stress in Fe–Mn–Si–Cr–Ni–C shape memory alloys. *Materials Science and Engineering: A*, *528*(3), 1125-1130.

Wen, Y. H., Li, N., and Xiong, L. R. (2005). Composition design principles for Fe–Mn–Si–Cr–Ni based alloys with better shape memory effect and higher recovery stress. *Materials Science and Engineering: A*, *407*(1-2), 31-35.

Wen, Y. H., Xie, W. L., Li, N., and Li, D. (2007). Remarkable difference between effects of carbon contents on recovery strain and recovery stress in Fe–Mn–Si–Cr–Ni–C alloys. *Materials Science and Engineering: A*, *457*(1-2), 334-337.

Wen, Y. H., Peng, H. B., Raabe, D., Gutiérrez-Urrutia, I., Chen, J., and Du, Y. Y. (2014). Large recovery strain in Fe-Mn-Si-based shape memory steels obtained by engineering annealing twin boundaries. *Nature communications*, *5*, 4964.